Rotation of Dust Structures in a Magnetic Field in a DC Glow Discharge

A. R. Abdirakhmanov, Zh. A. Moldabekov, S. K. Kodanova, M. K. Dosbolayev, and T. S. Ramazanov

***Abstract*— We present the experimental results on influence of an external magnetic field on the dust particles which were suspended in the strata of a glow discharge, where the magnetic field was created using a Helmholtz coil. Observations were made in the strata that located between the coils, under the coil, and above the coil. We observed an interesting behavior of dust particles, which was not previously reported. It was revealed that the dust structure rotates clockwise above the coil and counterclockwise under the coil, while the dust structure located between the coils does not rotate. Experiments were performed with both mono- and poly-disperse dust particles at $B \leq 28$ mT. The radial distribution of the angular velocity of dust particles, at the induction of the magnetic field 8, 13, and 19 mT, in different regions was measured. For explanation of the experimental results, we developed a simple theoretical model which shows that the direction of the rotation is determined by the radial component of the magnetic field induction.**

***Index Terms*— DC glow discharge, dusty plasma, magnetic field.**

I. Introduction

DUSTY plasmas can be found in different media, e.g., in planetary rings [1], and in the experiments on controlled fusion [2]. Charged dust particles can have a significant effect on plasma parameters and properties. Initially, investigation of dusty plasmas was motivated by the problem of controlling and removing dust particles from process plants. The study of the dust structures in the high-frequency (RF) discharge in a magnetic field was first reported in [3]–[6], and the results obtained using a stratified glow (dc) discharge in a magnetic field were reported in [7] and [8]. In [9]–[14], the properties of a dusty plasma in a strong magnetic field in an RF discharge and in a dc discharge, respectively, were studied. Investigation of dust particles dynamics in a magnetic field is of interest also for production of nanoparticles, e.g., the growth of nanoparticles in a magnetized chemically active discharge (Ar/C2H2) was investigated in [15].

In [7], a "rotational inversion" of plasma-dust structures was reported. At the present time, several mechanisms explaining this effect are known. The first one is the change in the radial ion flux due to the strengthening of magnetic field [16]. The second mechanism is the existence of an eddy current in strata [17]. In addition, Nedospasov [18], [19] has pointed out that the gas rotation due to the moment of Ampere force—which appears in the vicinity of solenoid end faces and in the narrowing of the cross section of the discharge channel—can have a significant impact on the dust structure. In [20], the theoretical models from [16] and [17] were tested experimentally. In particular, the influence of the edge effect of the solenoid on the dynamics of plasma-dust structures was investigated. For this purpose, a special modernized long solenoid was created, where the entire plasma area was located inside the magnetic field. It was obtained that the inversion of the rotation direction of dust structures is not due to the action of the edge effect.

In previous experiments—using a dc discharge—a diaphragm (an insert that narrows a discharge radius) was used [7], [8]. In this work, such a diaphragm was not used. Usually, the aforementioned diaphragm is used to get stable standing strata, with the position of the first standing stratum above the diaphragm (the inset). The latter also reduces the influence of the cathode spot on the discharge parameters. We found that a stable stratified glow discharge without a diaphragm can be realized by varying the discharge parameters. This is possible due to different locations of the electrodes and a smaller diameter of the discharge tube in comparison with that of used in the works reported in [7] and [8].

II. Experimental Setup

In order to study dust structures in an external magnetic field, we used experimental facilities with a dc stratified glow discharge. The experimental setup is a vertically oriented glass discharge tube with a length of 60 cm and a diameter of 3 cm. The top electrode is the anode, and the bottom is the cathode. Electrodes are made of copper in the form of a cone. The advantage of the cone-shaped electrode is a larger collecting surface, which creates the condition for better stability of the discharge. Electrodes are located in the lateral processes. This is necessary to prevent instability in the discharge. The scheme of the experimental setup is shown in Fig. 1. We performed experiments with both polydisperse and monodisperse particles. In the case of polydisperse particles, Al_2O_3 particles with the diameter in the range 1–6 μm and with random distribution in size were used. In our setup, the size of the particles which are levitated in stratum cannot be directly measured.

Manuscript received September 14, 2018; revised January 26, 2019; accepted March 12, 2019. Date of publication April 11, 2019; date of current version July 9, 2019. This work was supported by the Ministry of Education and Science of the Republic of Kazakhstan under Grant AP05133536 (2019). The review of this paper was arranged by Senior Editor T. Hyde. *(Corresponding author: A. R. Abdirakhmanov.)*

The authors are with the Institute of Experimental and Theoretical Physics, Al-Farabi Kazakh National University, Almaty 050040, Kazakhstan (e-mail: abdirakhmanov@physics.kz; zhandos@physics.kz; kodanova@physics.kz; merlan@physics.kz; ramazan@physics.kz).

This paper has supplementary downloadable material available at http://ieeexplore.ieee.org, provided by the authors.

Color versions of one or more of the figures in this paper are available online at http://ieeexplore.ieee.org.

Digital Object Identifier 10.1109/TPS.2019.2906051

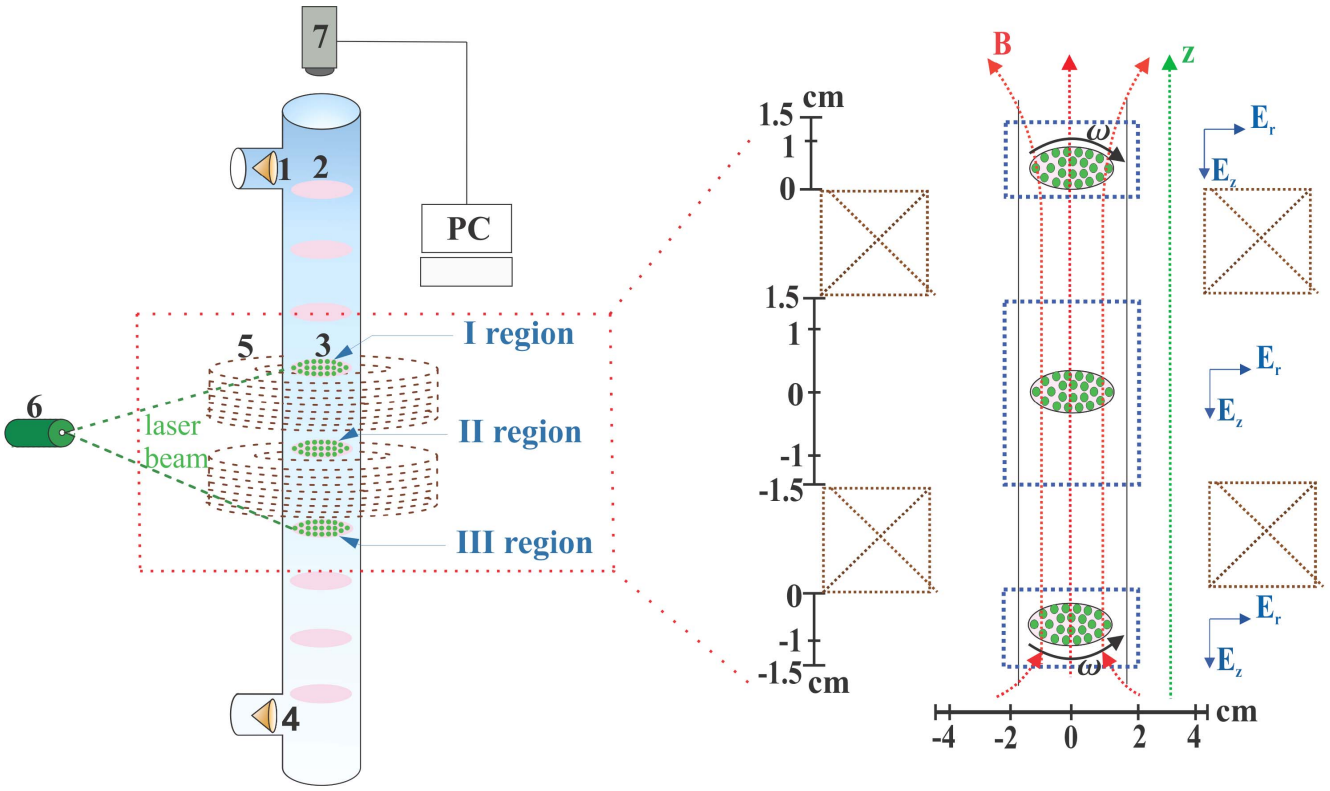

Fig. 1. Experimental setup. 1—anode, 2—stratum, 3—explored plasma-dust structures, 4—cathode, 5—Helmholtz coil, 6—laser for illumination, and 7—CCD camera.

Within one strata (in the case of polydisperse particles), heavy particles are located in a bottom part and light particles are located in an upper part of a strata. It is unclear if there is a major difference in the size of the particles in different stratification regions. However, as the configuration of the electrical field in strata is similar one to another [15], we think that the size of levitating dust particles should be similar in different strata. Taking into account uncertainties related to the random size distribution of the polydisperse particles, we have performed more experiments using melamin-formaldehid monodisperse particles with the diameter 2 μm.

In the case of polydisperse particles, the gas pressure was set to be 0.23 $\pm$ 0.01 torr, discharge current was 1.3 mA, and the induction of the magnetic field varied from 1 to 28 mT. At these parameters, standing strata without a diaphragm were created. Note that—at approximately these parameters—the dc discharge (containing polydisperse particles with the size similar to that of in this work) was investigated in detail in [16] and [17].

In the case of monodisperse particles, the gas pressure was 0.27 $\pm$ 0.01 torr, the discharge current was 1.5 mA, and the induction of magnetic field also varied in the range from 1 to 28 mT. Due to technical problems, we were unable to conduct experiments at significantly different values of pressures.

The dust particles (initially located inside the tube) were injected into the discharge by shaking the container holding dust particles (using a permanent magnet as a dust shaker). In our setup, we can change an output voltage of a high-voltage power supply (VS-22) in the range 0.6–3.8 kV. The visualization of the dust particles was carried out by means of illumination with a plane laser beam. In this setup, we used a solid-state laser with a diode-pumped green spectrum GL532TL-200 with a power of 0–200 mW. The scattered light was recorded by a CCD video camera KCB-340 (KOCOM) with a resolution of 640 $\times$ 480 pixel, with 250 frames/s. Video recording was performed on the top of the discharge tube through the optical window. A magnetic field was created using a Helmholtz coil, with a separation distance of 2.5 cm. The Helmholtz coil consists of two coils, wound from a high-strength heat-resistant coating of enameled copper wire with a diameter of 1.8 mm. The arrangement of Helmholtz coils is shown in Fig. 1. The coils have an inner diameter of 9 cm, outer diameter 14 cm, number of layers 14, and turns per layer 14. Magnetic induction depends on the current that flows through the copper wire. The maximum value of the applied magnetic field of 28 mT corresponds to a current of 9 A. To measure the magnetic field, we used a PHYWE teslameter from the PHYWE Company. The teslameter consists of a power source and a Hall probe. The latter was used to measure the axial and tangential components of the magnetic field induction.

The observations were made in the strata that were located between the coils, under the coil, and above the coil (see Fig. 1). Dust particles levitate simultaneously in all three regions. The recording of the structures in each region was done one by one, i.e, we observed the cloud in one of the regions and then moved the laser to other region.

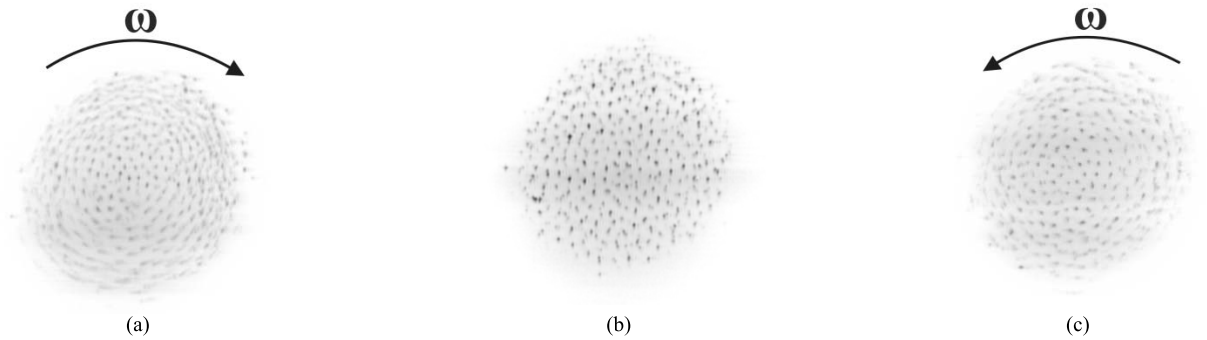

Fig. 2. Dust structures of the polydisperse particles in three regions (as indicated in Fig. 1). To illustrate the rotation in regions I and III and absence of the rotation in region II, several frames are imposed, so that the trace of dust particles can be seen. The rotation direction is shown for the clarity. The video files showing the rotation in regions I and III are provided as the Supplementary Material. (a) I region—the dust structure rotation is clockwise ($B \approx 15$ mT). (b) II region—the dust structure does not rotate ($B \approx 15$ mT). (c) III region—the dust structure rotates counterclockwise ($B \approx 15$ mT).

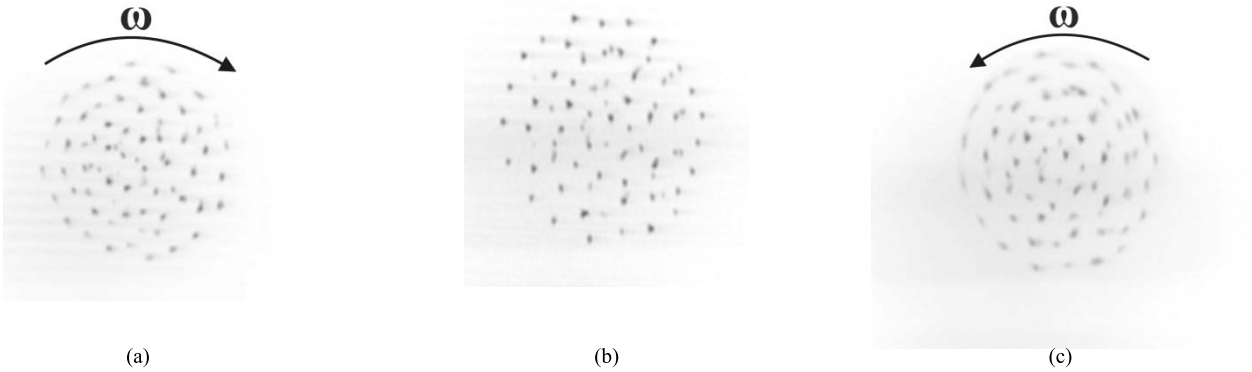

Fig. 3. Dust structures of the monodisperse particles in three regions (as indicated in Fig. 1), and rotation of them are illustrated. To illustrate the rotation in regions I and III and absence of the rotation in region II, several frames are imposed, so that the trace of dust particles can be seen. The rotation direction is shown for the clarity. (a) I region—the dust structure rotation is clockwise ($B \approx 15$ mT) (b) II region—the dust structure does not rotate ($B \approx 15$ mT). (c) III region—the dust structure rotates counterclockwise ($B \approx 15$ mT).

III. Results and Discussion

The views from top on the polydisperse and monodisperse dust structures are shown in Figs. 2 and 3, respectively. The diameter of the dust structures varies from approximately 3–3.5 mm. The observations were carried out in three regions (as indicated in Fig. 1). The first region (I)—where the dust structure was formed—is over the coil, the second region (II) is between the coils, and the third region (III) is under the coil. When the magnetic field is turned on, the dust particles in regions I and III had rotational motion on the horizontal plane. Clockwise and counterclockwise motions were observed in regions I and III, respectively, while the dust structure in region II did not rotate.

The motion of dust particles was recorded—in the horizontal section—by using the video camera. The angular velocity $\omega = \Delta\varphi/\Delta t$ was obtained by averaging the measurement results for several particles (about 10) in a zone, where $\Delta\varphi$ is the angular displacement of a particle over a period of time Δt. To find $\Delta\varphi$, the information about location of dust particles in frames separated by $\Delta t \sim 1$ s was used. The sign of the angular velocity of rotation was determined by the projection on the direction of the magnetic field, that is, when viewed from above, the counterclockwise rotation corresponded to the positive angular velocity.

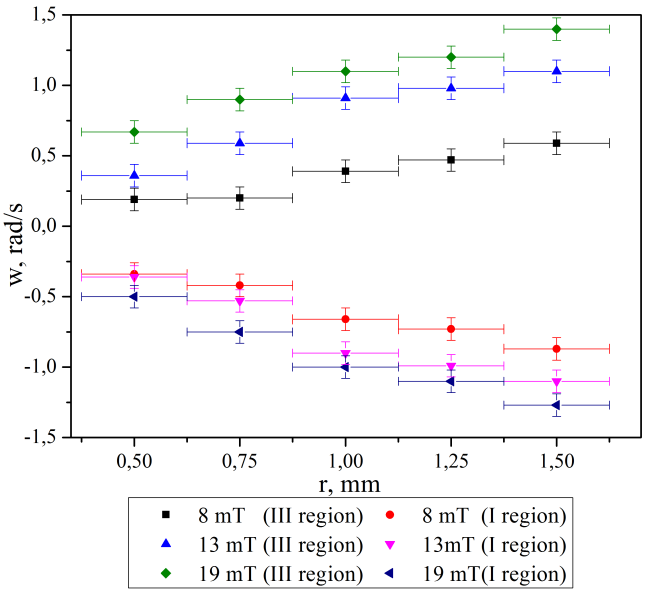

Fig. 4. Radial distribution of the angular velocity of the polydisperse dust particles in the dc glow discharge of Ar gas at 0.23 torr and current 1.3 mA.

For regions I and III, the radial distribution of the angular velocity of dust particles was measured at different values of the magnetic field induction (we considered 8, 13, and 19 mT).

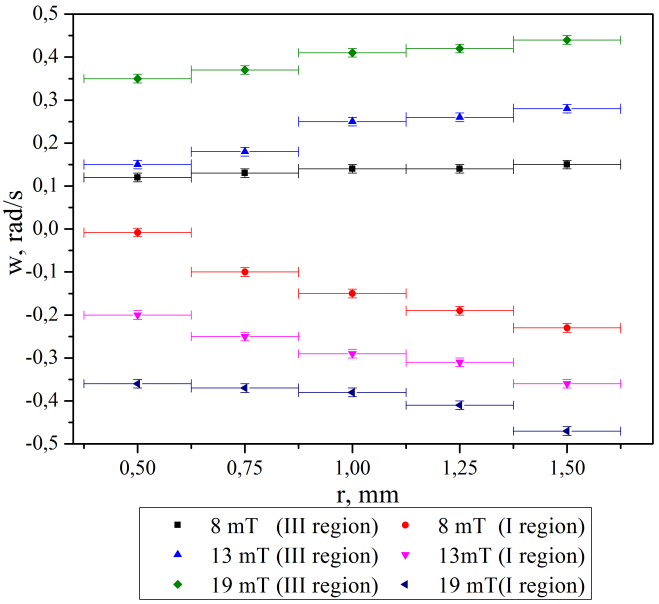

Fig. 5. Radial distribution of the angular velocity of the monodisperse dust particles in the dc glow discharge of Ar gas at 0.27 torr and current 1.5 mA.

The results for the polydisperse and monodisperse dust particles are shown in Figs. 4 and 5, respectively. Note that, the values of the magnetic field induction were measured along the z-axis passing through the center of the tube. From Figs. 4 and 5, it is evident that the dust structure rotates not as a rigid body, since the value of the angular velocity has a nonconstant distribution. The angular velocity increases with distance from the central part of the structure and with increase in the value of the magnetic field induction. As mentioned, the dust structure rotation direction in region I is opposite to that of in region III. The angular velocities of the monodisperse particles (at gas pressure 0.27 torr) are smaller than that of the polydisperse particles (at 0.23 torr). This may be understood as the result of the stronger friction by neutral particles. In addition, as the strength of magnetic field was increased, the reduction in size of the plasma in the radial direction (pinch effect) took place. This was evidenced by the loss of the dust particles, resulting in a decrease in the diameters of the structures from approximately 2.5–2 mm.

The magnetic induction $\vec{B}$ can be considered as the sum of the azimuthal $\vec{B}_{\parallel}$ (vertically along the tube) and radial $\vec{B}_{\perp}$ components (as illustrated in Fig. 1). In previous works with $B_{\perp} = 0$ and $\vec{B} \uparrow\uparrow \vec{E}_{\parallel}$, the rotational motion occurred due to an azimuthal drag force which appears as the result of the deviation of the radial component of the ion flux in a vertical magnetic field [6], [16]. In these works with $B_{\perp} = 0$ and $\vec{B} \uparrow\uparrow \vec{E}$, the direction of rotation was determined by the Lorentz force $\vec{E}_{\perp} \times \vec{B}$, where $\vec{E}_{\perp}$ is the radial electric field. In our experiment, in region II, we also had $B_{\perp} = 0$ and the dust structure did not rotate.

In region III, $B_{\perp} \neq 0$ is directed from the wall to the center. In region I, $B_{\perp} \neq 0$ is directed from the center to the wall (see Fig. 1). Clearly, in our experiment, the $\vec{E}_{\perp} \times \vec{B}$ induced ion flow cannot be the cause of the rotation as the direction of the rotation in regions I and III is opposite to each other. Therefore, it is expected that $\vec{E}_{\parallel} \times \vec{B}_{\perp}$ directed ion flow leads to the rotation of the dust particles. The azimuthal drift (flow) of ions can be estimated using the fluid equations

$$(\nu_i + \vec{v}_i \cdot \vec{\nabla})\vec{v}_i = \vec{E} + \vec{v}_i \times \vec{\Omega}_i \tag{1}$$

where $\vec{v}_i$ is the ion flow velocity, $\vec{\Omega}_i$ is the vector with absolute value given by the ion-cyclotron frequency and directed along the magnetic field induction, and ν_i is the ion-neutral collision frequency. In (1), we have neglected the ion pressure gradient and the centrifugal force (which is shown to be a safe approximation for considered plasma parameters [5]). Introducing an effective damping rate $\nu_i^* = \nu_i + V_r(d/dr) \approx \nu_i + V_r/L$ (with L being the characteristic length in the radial direction), Kaw *et al.* [5] derived a model for the description of the dust particles rotation for the case $B_{\perp} = 0$ and $\vec{B} \uparrow\uparrow \vec{E}_{\parallel}$. Similarly, for the case $B_{\perp} \neq 0$, from (1), we derive the azimuthal ionic flow velocity

$$v_{i\theta} = -\frac{F_r}{m}\frac{\Omega_i \sin\alpha}{\nu_i^2 + \Omega_i^2 \sin^2\alpha} \pm v_{iz}\frac{\nu_i \Omega_i \cos\alpha}{\nu_i^2 + \Omega_i^2 \sin^2\alpha} \tag{2}$$

where a plus (minus) sign is for region III (I), and α is the smallest angle between $\vec{B}$ and the unit vector $\vec{e}_r$ directed from the center of the tube toward the wall (in cylindrical system of coordinates with z-axis shown in Fig. 1). Index θ denotes the azimuthal component of the vector and z indicates the axial (along z axis) component of the vector.

Equation (2) is in agreement with the result of [5] in the case $\alpha = \pi/2$. The second term arises due to $B_{\perp} \neq 0$. We see that the second term in (2) has a negative sign in region I and positive sign in region III, explaining different rotation directions of the dust particles in these regions.

Following [5], the steady state of rotation of the dust particles can be formulated as the balance between drag by azimuthal ionic flow and friction by neutrals. From this condition, the azimuthal rotation velocity of a dust particle reads

$$v_{d\theta} \simeq \frac{n_i \sigma_{id}}{n_n \sigma_{nd}} v_{i\theta} \tag{3}$$

where $\sigma_{id}(\sigma_{nd})$ is the momentum transfer cross section for ion-dust particle (neutral atom-dust particle) collision, and $n_i(n_n)$ is the density of ions (atoms). In (3), it was assumed that temperatures of ions and neutrals are approximately equal to each other, i.e., $T_i \approx T_n$.

The second term on the right-hand side of (2) is absent in region II. In this region, the dust particles do not rotate and, therefore, the first term on the right-hand side can be neglected as being unable to induce dust particles rotation. For the estimation of the rotation frequency of the dust particles in regions I and III, taking into account that the electric field configuration in regions I–III is similar [21], [22], we neglect the contribution of the first term on the right-hand side of (2). Furthermore, let us take $\alpha = \pi/4$ for the estimation of the angular velocity of dust particles. Using characteristic values for the considered discharge parameters [21]–[23], we find $(n_i\sigma_{id})/(n_n\sigma_{nd}) \sim 10^{-7}$, $v_z \sim 10^2$ m/s. The rotation frequency then can be found using $\omega_d \approx v_{d\theta}/r_d$ (with r_d being

the distance from the center). We take $r_d \approx 1$ mm, and find for the monodisperse particle $\omega_d \approx 10^{-1} \div 10^{-2}$ rad/s, which is in a qualitative agreement with the experimental results.

IV. Conclusion

In our experiment, the dust structures in the first and third regions were under different configurations of the magnetic field lines. In the first region, the lines of the magnetic field induction have a divergent characteristic, and in the third region, a descending characteristic. Therefore, the dust structures in these regions rotate in opposite directions. We measured the dependence of the mean angular velocity on the induction of the magnetic field in different regions.

The main mechanism causing the rotation of dust particles is collisional interaction with the azimutal ionic flow. In the considered configuration of the magnetic and electric fields, the interplay between axial electric field and radial component of the magnetic field induction leads to the azimutal flow of ions. The divergent and descending characteristic of the magnetic field leads to different rotation directions of the dust particles; the latter is directed along $\overrightarrow{E_\parallel} \times \overrightarrow{B_\perp}$.

We plan to continue this research by considering discharge tubes with different diameters and different gas pressures. In addition, more accurate theoretical study and simulation of the observed processes should be done.

Finally, it should be mentioned that dust particles interaction (potential) under the impact of parallel electric and magnetic fields was studied theoretically (by simulation) in many previous works (see [24]). In contrast, such investigation of the case with crossed electric and magnetic fields is lacking. The presented experimental results show that an extension of the theoretical studies to the latter case is of importance.

References

[1] C. K. Goertz, "Dusty plasmas in the solar system," *Rev. Geophys.*, vol. 27, no. 2, pp. 271–292, May 1989.

[2] J. Winter, "Dust in fusion devices—Experimental evidence, possible sources and consequences," *Plasma Phys. Controlled Fusion*, vol. 40, pp. 1201–1210, Jun. 1998.

[3] N. Sato, G. Uchida, T. Kaneko, S. Shimizu, and S. Iizuka, "Dynamics of fine particles in magnetized plasmas," *Phys. Plasmas*, vol. 8, no. 5, pp. 1786–1790, 2001.

[4] U. Konopka, D. Samsonov, A. V. Ivlev, J. Goree, V. Steinberg, and G. E. Morfill, "Rigid and differential plasma crystal rotation induced by magnetic fields," *Phys. Rev. E, Stat. Phys. Plasmas Fluids Relat. Interdiscip. Top.*, vol. 61, p. 1890, Feb. 2000.

[5] P. K. Kaw, K. Nishikawa, and N. Sato, "Rotation in collisional strongly coupled dusty plasmas in a magnetic field," *Phys. Plasmas*, vol. 9, no. 2, p. 387, Feb. 2002.

[6] M. Puttscher and A Melzer, "Dust particles under the influence of crossed electric and magnetic fields in the sheath of an RF discharge," *Phys. Plasmas*, vol. 21, Nov. 2014, Art. no. 123704.

[7] V. Y. Karasev, E. S. Dzlieva, A. Y. Ivanov, and A. I. Eikhvald, "Rotational motion of dusty structures in glow discharge in longitudinal magnetic field," *Phys. Rev. E, Stat. Phys. Plasmas Fluids Relat. Interdiscip. Top.*, vol. 74, Dec. 2006, Art. no. 066403.

[8] M. M. Vasiliev, L. G. D'yachkov, S. N. Antipov, R. Huijink, O. F. Petrov, and V. E. Fortov, "Dynamics of dust structures in a DC discharge under action of axial magnetic field," *Europhys. Lett.*, vol. 93, Jan. 2011, Art. no. 15001.

[9] E. Thomas, Jr., B. Lynch, U. Konopka, R. L. Merlino, and M. Rosenberg, "Observations of imposed ordered structures in a dusty plasma at high magnetic field," *Phys. Plasmas.*, vol. 122, no. 3, pp. 030701-1–030701-4, 2015.

[10] T. Hall, E. Thomas, Jr., K. Avinash, R. Merlino, and M. Rosenberg, "Methods for the characterization of imposed, ordered structures in MDPX," *Phys. Plasmas*, vol. 25, Oct. 2018, Art. no. 103702.

[11] E. Thomas, Jr., U. Konopka, B. Lynch, S. Adams, S. LeBlanc, and L. Robert, "Quasi-discrete particle motion in an externally imposed, ordered structure in a dusty plasma at high magnetic field," *Phys. Plasmas*, vol. 22, Nov. 2015, Art. no. 113708.

[12] S. Jaiswal, T. Hall, S. LeBlanc, R. Mukherjee, and E. Thomas, Jr., "Effect of magnetic field on the phase transition in a dusty plasma," *Phys. Plasmas*, vol. 24, Nov. 2017, Art. no. 113703.

[13] V. Karasev, E. Dzlieva, S. Pavlov, L. Novikov, and S. Maiorov, "The rotation of complex plasmas in a stratified glow discharge in the strong magnetic field," *IEEE Trans. Plasma Sci.*, vol. 46, no. 4, pp. 727–730, Apr. 2018.

[14] S. I. Pavlov *et al.* "Observation of the dynamics of the dust structure in a dust trap in a double electric layer in a magnetic field up to 10,000 G," *Contrib. Plasma Phys.*, Feb. 2019. doi: 10.1002/ctpp.201800142.

[15] l. Couëdel *et al.*, "Influence of magnetic field strength on nanoparticle growth in a capacitively-coupled radio-frequency Ar/C_2H_2 discharge," *Plasma Res. Express*, vol. 1, no. 1, Feb. 2019, Art. no. 015012.

[16] E. S. Dzlieva, V. Y. Karasev, S. I. Pavlov, M. A. Ermolenko, L. A. Novikov, and S. A. Maiorov, "The dynamics of dust structures under magnetic field in stratified glow discharge," *Contrib. Plasma Phys.*, vol. 56, pp. 197–203, Apr. 2016.

[17] E. S. Dzlieva, V. Y. Karasev, and S. I. Pavlov, "Detection of eddy current in the striation," *Europhys. Lett.*, vol. 110, no. 5, Jun. 2015, Art. no. 55002.

[18] A. V. Nedospasov, "Motion of plasma-dust structures and gas in a magnetic field," *Phys. Rev. E, Stat. Phys. Plasmas Fluids Relat. Interdiscip. Top.*, vol. 79, Mar. 2009, Art. no. 036401.

[19] A. V. Nedospasov and N. V. Nenova, "Gas rotation in discharge with moving strata in longitudinal magnetic field," *Europhys. Lett.*, vol. 108, Nov. 2014, Art. no. 45001.

[20] A. R. Abdirakhmanov, M. K. Dosbolayev, and T. S. Ramazanov, "The gas discharge dusty plasma in a uniform magnetic field," in *Proc. AIP Conf.*, vol. 1925, Jan. 2018, Art. no. 020007.

[21] G. I. Sukhinin, A. V. Fedoseev, T. S. Ramazanov, R. Z. Amangaliyeva, M. K. Dosbalayev, and A. N. Jumabekov, "Non-local effects in a stratified glow discharge with dust particles," *J. Phys. D, Appl. Phys.*, vol. 41, Nov. 2008, Art. no. 245207.

[22] G. I. Sukhinin, A. V. Fedoseev, T. S. Ramazanov, K. N. Dzhumagulova, and R. Z. Amangaliyeva, "Dust particle charge distribution in a stratified glow discharge," *J. Phys. D: Appl. Phys.*, vol. 40, p. 7761, Nov. 2007.

[23] T. S. Ramazanov, N. K. Bastykova, Y. A. Ussenov, S. K. Kodanova, K. N. Dzhumagulova, and M. K. Dosbolayev, "The behavior of dust particles near Langmuir probe," *Contrib. Plasma Phys.*, vol. 52, p. 110, Feb. 2012.

[24] P. Ludwig *et al.*, "Non-Maxwellian and magnetic field effects in complex plasma wakes," *Eur. Phys. J. D*, vol. 82, p. 72, May 2018.

Authors' photographs and biographies not available at the time of publication.